Principles and Progress in Ultrafast Multidimensional Nuclear Magnetic Resonance

Mor Mishkovsky and Lucio Frydman

Department of Chemical Physics, Weizmann Institute of Science, 76100 Rehovot, Israel;
email: Lucio.Frydman@weizmann.ac.il

Key Words

NMR spectroscopy, multidimensional acquisitions, ultrafast methods, spatial encoding, hyperpolarized samples

Abstract

Multidimensional acquisitions play a central role in the progress and applications of nuclear magnetic resonance (NMR) spectroscopy. Such experiments have been collected traditionally as an array of one-dimensional scans, with suitably incremented delay parameters that encode along independent temporal domains the nD spectral distribution being sought. During the past few years, an ultrafast approach to nD NMR has been introduced that is capable of delivering any type of multidimensional spectrum in a single transient. This method operates by departing from the canonical nD NMR scheme and by replacing its temporal encoding with a series of spatial manipulations derived from magnetic resonance imaging. The present survey introduces the main principles of this subsecond approach to spectroscopy, focusing on the applications that have hitherto been demonstrated for single-scan two-dimensional NMR in different areas of chemistry.

1. INTRODUCTION

MRI: magnetic resonance imaging

Fourier transform (FT): the mathematical procedure that enables one to discern which frequency contributions compose a time-dependent signal response function

Free induction decay: traditional term used to denote time-domain signals of the kind described in Equation 1 and arising upon exciting a spin ensemble in an NMR experiment

T_2: spin-spin relaxation time, describing the decoherence lifetimes of the spins' signal following their excitation into a transverse evolution plane

Nuclear magnetic resonance (NMR) is a spectroscopic technique based on monitoring the precession of spin-endowed atomic nuclei when placed in a strong external magnetic field. With its origin in curiosity-driven investigations about the nature of quantum mechanical phenomena, NMR has over the years transformed into an indispensable applied tool that impacts a remarkably wide range of scientific disciplines (1). High-resolution NMR of dissolved molecules, for example, serves as the eyes of chemists involved in organic, pharmaceutical, and natural-products research (2). When employed in combination with high-resolution solid-state techniques, NMR provides a unique window to study the chemical structure of challenging heterogeneous materials, including polymorphic mixtures, polymers, glasses, and catalysts (3). It is one of the few methods available for determining the structure and the dynamics of proteins and nucleic acids in their native solution state at individual, site-resolved levels (4). Moreover, even if concealed under different names [e.g., magnetic resonance spectroscopy or magnetic resonance imaging (MRI)], NMR has evolved into a widely used in vivo tool capable of diagnosing and imaging malignancies, evaluating metabolic status, angiographing noninvasively, and revealing the activation of human brains even to the smallest of stimuli (5, 6).

Despite this outstandingly wide scope of applications, broadly speaking, one common measurement protocol underlies all these different uses of the quantum-mechanic spin-precession phenomenon: the pulsed Fourier transform (FT) NMR method, whose purpose is to measure inductively the different Bohr evolution frequencies allowed to the spin ensemble under observation within its quantized energy manifold (1–7). These in turn are governed by isotropic shift or J-coupling interactions in liquid-state experiments, by these couplings plus a variety of spin anisotropies when dealing with solids, and by a combination of the above plus external ad hoc fields in the case of NMR imaging. Regardless of which parameters or interactions are actually sought, NMR extracts the frequency distributions originated by these couplings by monitoring the responses that they impart on the spins' time evolution. The result arising in these measurements upon subjecting spins to an excitation impulse is the so-called free induction decay, a signal (voltage) given by a weighted sum of oscillating functions,

$$S(t) = \sum_{\text{acting}\,\Omega} I(\Omega) \exp(i\Omega t) \exp(-t/T_2), \tag{1}$$

defined by the allowed single-quantum spectral distribution of allowed transitions $I(\Omega)$, as well as by a T_2 relaxation decay. $S(t)$ can then clearly provide the $I(\Omega)$ spectrum sought by FT versus the single variable t, defining the time domain that supports it.

Although pulsed NMR experiments initially involved only this kind of data collection, as a function of a single time axis (8), it was soon realized that significant benefits could result by correlating the spins' evolution along multiple time domains (9, 10). These nD NMR experiments would then not just measure but also correlate and separate different contributions to the overall spin-precession frequencies; this could improve the resolution of the experiment, as well as extract information that would be simply unavailable in the single-quantum one-dimensional (1D) trace. The canonical scheme for such experiments follows Jeener and Ernst's seminal 2D NMR proposal, which laid the foundations for multidimensional spectroscopy based on the four blocks (9, 10)

$$\text{Preparation} - \text{Evolution}\,(t_1) - \text{Mixing} - \text{Acquisition}\,(t_2). \tag{2}$$

By suitable incrementation of the t_1 and t_2 time variables, an NMR experiment of this kind can then yield a 2D time-domain signal,

$$s(t_1, t_2) = \int_{all\,\Omega_2} d\Omega_2 \left[\int_{all\,\Omega_1} d\Omega_1 I(\Omega_1, \Omega_2) e^{i\Omega_1 t_1} e^{-t_1/T_2} \right] e^{i\Omega_2 t_2} e^{-t_2/T_2}, \tag{3}$$

from which correlations between so-called indirect- and direct-domain NMR frequencies Ω_1 and Ω_2 can be extracted by 2D FT analysis:

$$I(\nu_1, \nu_2) \propto \int_{\text{all } t_2} dt_2 \left[\int_{\text{all } t_1} dt_1\, S(t_1, t_2) e^{-i\nu_1 t_1} \right] e^{-i\nu_2 t_2}. \tag{4}$$

At first glance, this approach to the retrieval of $I(\Omega_1, \Omega_2)$ appears to be a simple extension of the 1D time-domain NMR experiment to two dimensions. The multiple times involved in these acquisitions, however, actually possess different origins. t_2 is a physical acquisition time along which the signal is directly digitized, akin to the t time involved in the 1D NMR free induction decay of Equation 1; the spins' behavior along this direct-domain axis therefore can be characterized by FT of data digitized throughout a single-scan experiment. The remaining time axes of the experiment, however, cannot be sampled in the same fashion. This is resolved in the Jeener-Ernst paradigm by monitoring these domains indirectly, i.e., by carrying out N_i discrete incrementations of certain time delays t_i within the sequence throughout a series of independent experiments. Herein lies the brilliance, yet also a potential weakness, of this kind of acquisition. Indeed, regardless of sensitivity considerations, nested encoding schemes such as the one represented by Equation 2 require monitoring tens or hundreds of independent increments along each of the $n-1$ indirect-domain time axes to properly characterize its internal evolution frequencies. Moreover, because each point along these $n-1$ indirect time domains is associated with an independent signal acquisition, this results in an exponential increase of the minimum experimental acquisition time with dimensionality n. The unambiguous gains resulting from expanding NMR from a 1D to an nD experiment may therefore come at a price.

Driven by this reality, and stimulated by an increasing reliance of all the above-mentioned contemporary NMR applications on high-dimensional experiments, a growing number of alternatives that depart from the traditional sampling principles embodied by Equation 2 have emerged during the past few years (11, 21). These include routes that process the acquired data by non-Fourier methods (13–16), acquisitions that incorporate frequency-based manipulations (17), and accordioned derivations (18) whereby multiple indirect-domain time delays are incremented simultaneously (19–21). Among these new proposals is also an ultrafast approach, departing both from the traditional temporal encoding and from the alternatives just mentioned, that enables the acquisition of arbitrary multidimensional data sets within a single scan without requiring any a priori information (22–24). At the heart of this proposal is a departure from the classical Jeener-Ernst serial incrementation scheme, which is replaced by a parallel encoding of the indirect-domain time information along a spatial dimension. This review discusses the basic features and potential applications of this ultrafast NMR method, particularly as it is used within the context of rapid 2D NMR acquisitions. We summarize first the physical principles underlying ultrafast 2D NMR, continue with an overview of some potential applications of this method, discuss its combination with a variety of schemes enabling its extension to higher dimensions, and conclude by reviewing additional applications that have been recently demonstrated based on the spatial-encoding concepts on which ultrafast NMR spectroscopy relies.

2. SPATIAL ENCODING AND THE SINGLE-SCAN ACQUISITION OF 2D NUCLEAR MAGNETIC RESONANCE SPECTRA

Ultrafast 2D NMR methods depart from traditional schemes in that, instead of triggering the indirect-domain evolutions homogenously, for all sites and positions within the analyzed sample at once, they encode the evolution frequencies being sought in a spatially heterogeneous fashion. Several alternatives have been proposed for achieving such heterogeneous evolution (22, 25–30),

a majority of which impart different evolution durations prior to the mixing period on spins positioned at different coordinates within the sample. All these schemes share the application of a train of either continuous or discrete frequency-swept radiofrequency (RF) pulses, acting in combination with suitably echoed magnetic field gradients. These procedures are tuned so as to impart indirect-domain evolution times proportional to the spins' coordinate along a particular direction z. In other words, they rely on a spatial encoding of the spin interactions, whereby the indirect-domain evolution time of a 2D NMR experiment is made $t_1 \approx Cz$, where C is a spatio-temporal constant under the experimentalist's control. (This C parameter is usually given by $\frac{t_1^{max}}{L}$, the maximum t_1 evolution time imparted, divided by the overall sample length L.) The evolution coupling parameters Ω_1 being sought thus impart over these periods an effective spatially dependent precession phase $\phi(z) \approx \Omega_1 t_1 = C\Omega_1 z$. It follows that within the framework of a Bloch space in which the spins' magnetizations precess within a common rotating frame (**Figure 1**) every chemical site within the sample subtends a shift-induced helical pattern along the z spatial coordinate:

$$M_x(z) + i M_y(z) \propto \frac{I(\Omega_1)}{L} \exp(iC\Omega_1 z) \exp(-Cz/T_2). \tag{5}$$

The helical winding of magnetizations represented by this equation is characterized by a pitch depending on the Ω_1 parameter one is attempting to measure but in general does not lead to any net observable signal as these helices are characterized by a destructive interference among their constituent spin packets when considered over a macroscopic sample. Nevertheless, their encoded information can be preserved throughout the various coherent mixing processes involved in a 2D NMR pulse sequence and, at a final acquisition stage, can be read out by applying a z-dependent gradient acting in combination with the data sampling. Indeed, field gradients have the ability to wind and unwind spin-magnetization patterns of their own according to

$$M_x \xrightarrow{\gamma Gz \cdot t} M_x \cos(\gamma Gzt) + M_y \sin(\gamma Gzt)$$
$$= M_x \cos(kz) + M_y \sin(kz). \tag{6}$$

Under suitable conditions, therefore, these succeed to successively unwind the various helices that were subtended by the individual chemical sites, leading to observable echoes arising from constructive interference phenomena among spins positioned throughout the sample L (**Figure 1**). Moreover, as the timing of such echoes depends on the strengths of the Ω_1 internal interactions that created each site's winding, this allows one to map the indirect-domain spectral information being sought by monitoring the positions of the resulting echo peaks. Mathematically, these spectral peak positions are characterized by the values taken by the wave numbers $k = \gamma_a \int_0^t G_a(t')dt'$, representing the action of the unwinding acquisition gradient G_a. Assuming that this MRI-like acquisition process begins in a spatially encoded magnetization pattern of the kind described by Equation 5, the integral of the observable signal over the sample length is then

$$S[k(t)] \approx \sum_{\Omega_1} I(\Omega_1) \int_L \exp[iC\Omega_1 z] \exp[-Cz/T_2] \exp[ik(t)z]dz$$
$$\approx \sum_{\Omega_1} I(\Omega_1)\delta[C\Omega_1 + k]. \tag{7}$$

This latter spectral sum includes well-behaved δ-functions such as *sinc*-, Lorentzian- or Gaussian lineshapes, leading to peaks whenever $-k/C$ matches an existing precession frequency. This ratio therefore becomes the equivalent, in this kind of experiment, to the indirect-domain frequency scale ν_1 in a conventional 2D acquisition.

A procedure such as the one summarized in **Figure 1** allows one to read out an NMR spectrum with the aid of a gradient-driven action—without the use of a numerical FT. A special feature of
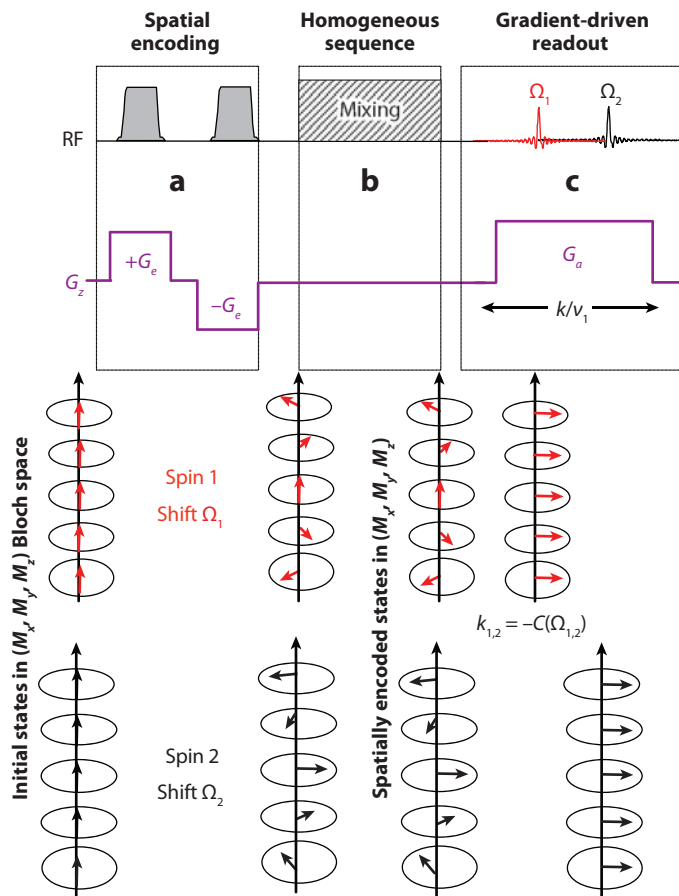
Figure 1

Imparting and reading out NMR spectral data by gradient-driven processes. (*Top panel*) A summary of the pulses and gradients applied to the spins. (*Bottom panel*) The idealized behavior imparted by these manipulations on two chemically inequivalent sites, each represented by an array of magnetization vectors as a function of their spatial z coordinates throughout the sample. (*a*) Spatial-encoding stage incorporating frequency-swept pulses and suitably refocused magnetic field gradients, G_e. The radiofrequency (RF) achieves a sequential excitation of spins along the direction of the gradient; because these are applied in a sign-alternating fashion, no phase related to the spatial position of spins is retained. The result is a shift-driven winding of the magnetizations along the gradient's direction (*bottom panel*). (*b*) This can be followed by conventional, homogenous sequences, for instance, those involved in arbitrary mixing processes. (*c*) Finally, data are collected while in the presence of an acquisition gradient, G_a, capable of unwinding the shift-induced magnetization spirals encoded during the excitation. The sharp echoes that are then generated unveil an array of peaks, delivering the NMR spectrum that acted on the spins during the stage shown in panel *a*.

such gradient-driven readout is that it can be implemented over a very short time, on the order of $T_a \approx t_1^{\max} \frac{2\pi \, SW_1}{\gamma_a \, G_a \, L}$, where SW_1 denotes the window of spectral frequencies one is seeking to characterize. These gradient effects can then be reversed immediately, simply by reversing the currents flowing through the gradient's amplifier, and can therefore be repeated multiple times over the course of a t_2 direct-domain acquisition time. This constitutes the second principal ingredient enabling the completion of the 2D experiment within a single scan: By rapidly alternating the sign of the decoding acquisition gradients, one can observe the $I(\Omega_1)$ spectrum repetitively and

a Oscillating-gradient acquisition

b Rearrangement and processing
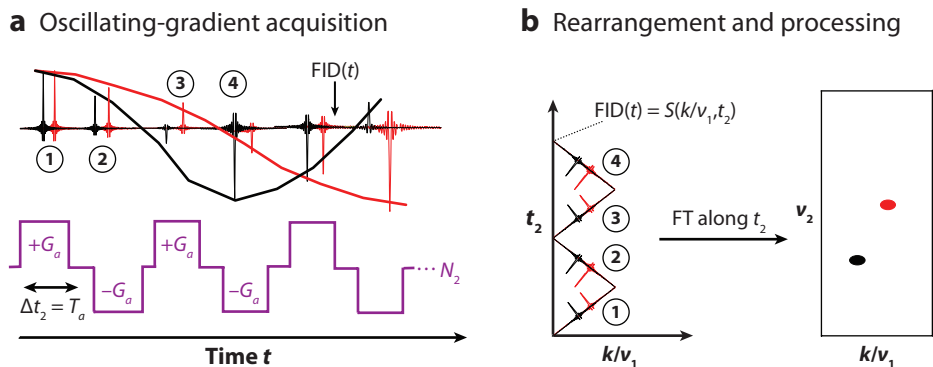
Figure 2

The extension of the single gradient–driven refocusing process illustrated in **Figure 1** to a multi-echo process capable of yielding full 2D NMR spectra within a single scan. (*a*) By performing multiple, rapid $\pm G_a$ oscillations, one can read out the spatially encoded indirect-domain spectrum $I(\Omega_1)$ many (N_2) times separated by relatively short intervals $\Delta t_2 = T_a$. The phase modulation then affecting the different echoes (*continuous lines*) is given by their respective direct-domain evolution frequencies Ω_2. (*b*) A full 2D NMR spectrum can therefore be obtained by rearranging the single-scan interferogram $I(k/\nu_1, t_2)$ represented by this free induction decay (FID) into its proper position within a 2D place, followed by its 1D Fourier transform (FT) as a function of $t = t_2$.

thereby monitor the phase modulation of the indirect-domain frequency peaks arising as a function of a detection time t_2. The time-domain signal $S(t)$ arising during the course of such an oscillating-gradient procedure thereby constitutes a 2D interferogram in the space subtended by the $\nu_1 = -k/C$ indirect-domain frequency axis and the $t_2 = t$ direct-domain acquisition time. Signals collected throughout this process and rearranged into their proper positions within such mixed frequency-/time-domain space can therefore lead to the desired 2D NMR spectrum if these echo signals are subjected to a final 1D FT process along the direct domain (**Figure 2**), all of this within a single scan.

3. POTENTIAL APPLICATIONS OF ULTRAFAST 2D NUCLEAR MAGNETIC RESONANCE

Further details underlying ultrafast NMR's spatial encoding and ways to implement such processes in contemporary NMR commercial hardware have been summarized recently in a comprehensive article (31). Therefore, we turn to a discussion of some potential applications and extensions that have been demonstrated based on this new approach to the single-transient collection of 2D NMR spectra.

3.1. Real-Time Ultrafast 2D Nuclear Magnetic Resonance of Samples Subject to Constant Flow

The capability of gaining structural information using 2D NMR transforms the single-scan approach described above into a potential candidate for identifying compounds and tracking chemical separations in real time. Indeed the past decade has witnessed a growing number of applications that use NMR spectroscopy to monitor compounds passing through its main observation coil, both as a metabonomics diagnostic tool (32) and in combination with liquid-chromatography procedures (33). When considering this kind of NMR observation, two main options arise: One
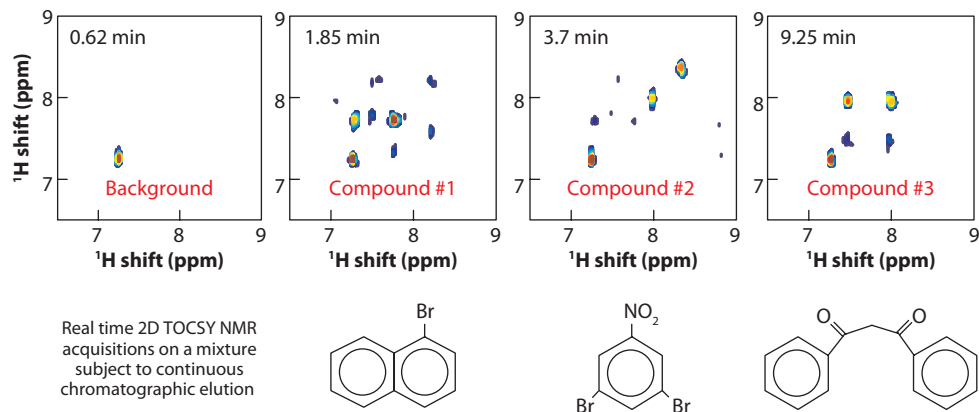
Figure 3

Real-time identification of mixed components subject to a continuous flow separation via 2D ultrafast ^{1}H total correlation–spectroscopy NMR (35). 2D NMR spectra were constantly acquired 32 s apart over a 15-min elution period; the figure concentrates on spectra corresponding to the drawn compounds appearing at the indicated elution times.

involves performing the measurements in a stopped-flow mode, whereby fractions are collected separately and inserted one by one into the NMR spectrometer for individual examination; the other involves monitoring the NMR spectra as analytes flow continuously through the observation coil. The latter experimental setup is more amenable to analyzing the large number of samples that one needs to monitor in either metabolic profiling or analytical separation applications, yet this flow mode limits its applicability to the collection of relatively short 1D experiments. Ultrafast 2D analyses, conversely, could open new possibilities toward the application of multidimensional NMR during the few seconds that samples typically spend within the NMR observation coil under typical elution conditions. In this context, given sufficient spectral sensitivity, the ultrafast 2D NMR protocol can measure homonuclear ^{1}H total correlation spectroscopy spectra (7, 34) of samples subjected to continuous flow through the NMR sample coil (**Figure 3**); further applications of these principles are envisioned.

3.2. Following Chemical and Biophysical Transformations by Ultrafast 2D Nuclear Magnetic Resonance

Another opportunity that may arise from rapid 2D NMR approaches concerns the possibility of monitoring chemical and/or biophysical transformations in real time. In fact, NMR spectroscopy offers a number of different avenues toward monitoring dynamic chemical and biophysical process (36–39). We can gain insight into kinetics occurring on fast (10^{-7}–10^{-3} s) timescales through a variety of relaxation time measurements, and environmental changes in the 10^{-2}–10^0 s range can be revealed by lineshape variations. However, longer timescales could be probed directly by monitoring changes in the appearance of 1D or 2D NMR spectra as a function of time, a standard approach for examining the nonequilibrium kinetics of chemical, biophysical, and in vivo processes (5, 38, 39). The timescales of conventional 2D NMR approaches, however, are not ideally suited to this kind of determination owing to their intrinsic multiscan acquisition modes; by shortening the minimum times required to complete the collection of the 2D NMR data, ultrafast methods could help alleviate this limitation. The data in **Figure 4** illustrate this ability with a series of 2D

Total correlation spectroscopy: a common type of homonuclear 2D experiment revealing connectivities between neighboring sites
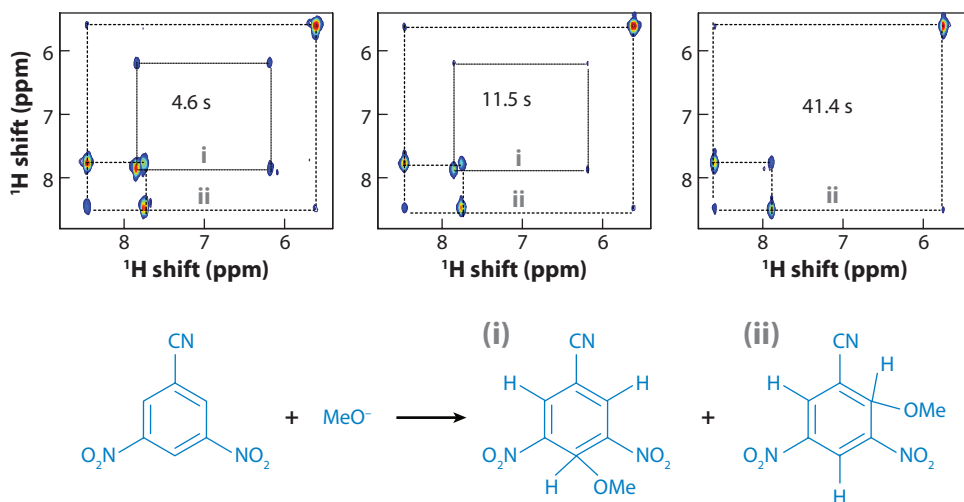
Figure 4

Real-time monitoring of a chemical reaction using ultrafast 2D total correlation spectroscopy NMR (40), illustrating the appearance of compounds (*bottom*) at the indicated times since triggering the reaction inside the NMR magnet. Both reactants were prepolarized prior to the reaction: One reactant was loaded into the 5-mm NMR tube, whereas the other was held within a capillary prior to its sudden injection.

NMR snapshots collected while a chemical reaction was triggered in situ within the NMR tube. Data acquisition in this kind of experiment began slightly before triggering the chemical process, and a series of 2D total correlation spectroscopy NMR spectra recorded every 2.3 s could reflect even transient stages of the ensuing Messenhimer complexation reaction (40).

If and when sensitivity suffices, biophysical transformations such as H/D exchange processes or folding events could also become amenable to this kind of measurement. In these biomolecular cases (in which sensitivity is always a challenge), it is often convenient to couple the ultrafast 2D protocol with other acquisition methods capable of minimizing the experiment's recycle delay and thereby maximize the number of 2D NMR frames available per unit acquisition time. One such recent proposal is the band-selective, optimized flip-angle, short-transient, heteronuclear multiple-quantum correlation NMR experiment (41, 42), which enables the reduction of the interscan repetition delay down to ≤100 ms while preserving high sensitivity by relying on an accelerated spin-lattice relaxation imparted from a selective excitation in combination with optimized flip angles to enhance the steady-state signal arising from the excited spins (43–45). This in return allows the recording of conventionally sampled 2D ^1H-^{15}N or ^1H-^{13}C correlation spectra within minimal experimental times of just several seconds. Moreover, if combined with ultrafast 2D NMR, this methodology can yield spectra at very high frame rates, compatible with the continuous following of biophysical processes. **Figure 5** illustrates an example of these spectra (46), with an H/D exchange process followed under experimental conditions that combine the very short interscan delay afforded by the optimized flip-angle protocol, with the single-scan capabilities of ultrafast NMR. This method is capable of collecting 2D NMR correlation spectra at ≈1-mM protein concentrations with frame rates of approximately 1 Hz; this could become an important aid in studying subsecond processes in which peak positions or intensities change owing to protein or nucleic acid folding, binding, or dynamics.

Heteronuclear multiple-quantum correlation: a common 2D NMR approach for determining the connectivity between heteronuclear pairs (e.g., ^1H and ^{15}N)
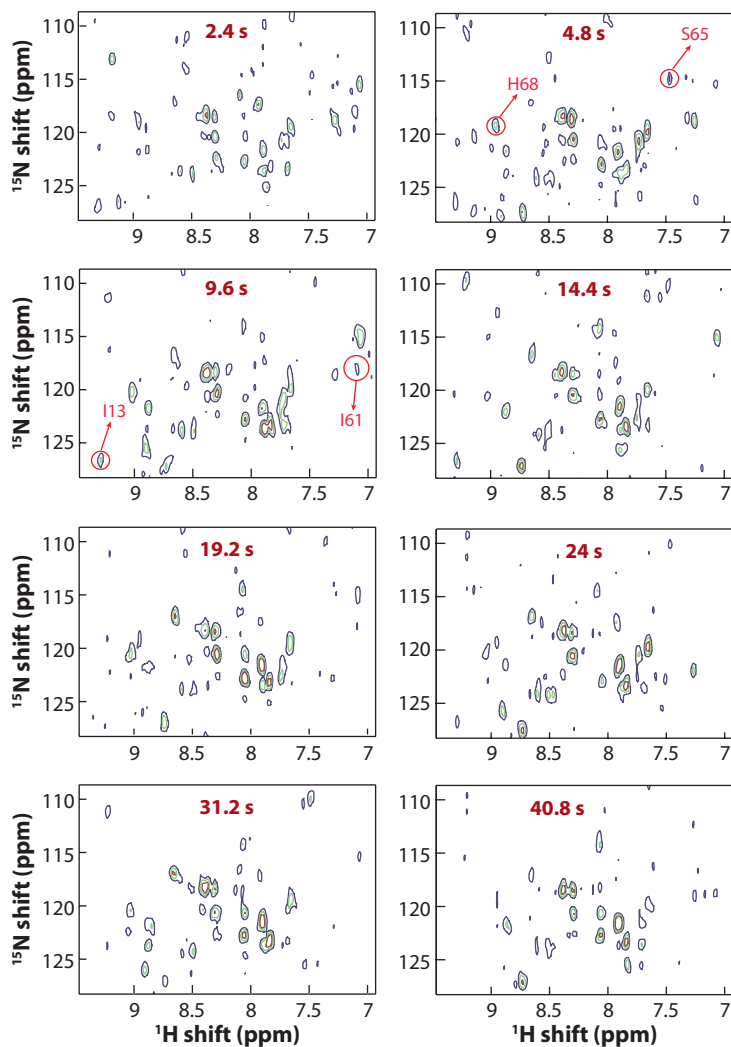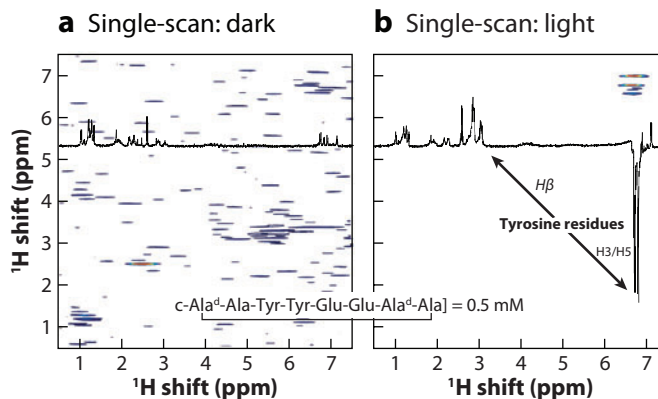
Figure 5

Representative series of real-time 2D ultrafast heteronuclear multiple-quantum correlation NMR spectra
recorded on an ubiquitin solution, using the band-selective, optimized-flip-angle, short-transient protocol,
following the dissolution of an initially fully protonated lyophilized powder onto a D_2O-based buffer as a
function of the time delay elapsed since the dissolution (46). The repetition time between full recording was
~2.4 s, and the data were monitored over a 20-min interval. Red circles indicate selected NH resonances
that rapidly disappear owing to the H → D exchange.

3.3. Ultrafast 2D Nuclear Magnetic Resonance on Prepolarized Samples

In recent years, we have witnessed the emergence of a variety of NMR prepolarization methods
capable of building up nuclear polarizations that exceed their thermal counterparts by several
orders of magnitude (47–50). In many instances, these methodologies are constrained to extract
their superspectra within a single or at most a few transients, making them poor starting points
for conventional 2D NMR experiments requiring the collection of a large set of scans. Such
a scenario presents another instance in which new possibilities could arise through the use of

**a** Single-scan: dark **b** Single-scan: light

Figure 6

Potential benefits resulting from combining chemically induced dynamic nuclear polarization (CIDNP) prepolarization and ultrafast 2D methods. Both panels illustrate single-scan 2D total correlation spectroscopy ^{1}H NMR spectra recorded on a cyclic octapeptide dissolved in D_2O at a 0.5-mM concentration. (*a*) Spectrum under standard conditions. (*b*) Spectrum resulting from pre-irradiating the sample for 0.5 s using a 480-nm light source (2W), generating a CIDNP enhancement of tyrosine's aromatic protons (52).

ultrafast 2D NMR methodologies. An early example of such an integration was the use of chemically induced dynamic nuclear polarization (CIDNP), a prepolarization process involving the light irradiation of a suitable photoexcitable molecule (51). When this irradiation is carried out in the presence of a suitable peptide or protein sample, the generated radicals may have the capability of affecting the steady-state polarization of the nuclear spins of certain aromatic residues (e.g., tryptophan, tyrosine, and histidine) via nuclear-electron hyperfine interactions. As usual, when implementing NMR studies on peptides or proteins, it would be desirable to carry out this sensitivity-enhancement procedure while spreading the affected resonances throughout a 2D frequency spectrum. CIDNP, however, has a limited compatibility with 2D NMR owing to significant photobleaching effects that set in after the first few light irradiation cycles. Ultrafast 2D NMR can help complete photo-CIDNP acquisitions on such prepolarized samples within a single scan and thus avoid such complications altogether; **Figure 6** shows a preliminary step in that direction with a single-scan 2D total correlation spectroscopy spectrum acquired at submillimolar concentrations following a brief period of CIDNP polarization enhancement (52).

An even more promising integration combines dynamic nuclear polarization (DNP) as the magnetization build-up process, with heteronuclear ultrafast 2D correlation spectroscopies. DNP is one of the earliest (53–55) and arguably one of the most general hyperpolarization mechanisms, as it only requires the irradiation of a small amount of free radical mixed with the target molecule to achieve its goals. Although the DNP process itself is usually carried on a frozen glass, one can now rapidly melt and transfer such a hyperpolarized mixture into a conventional NMR spectrometer, thereby benefiting from a very large signal enhancement also in the liquid state (56, 57). The availability of a commercial instrument capable of performing this single-shot DNP hyperpolarization of liquid samples has caused substantial excitement in the fields of NMR and MRI (58–62). Once again, the ultrafast approach seems well suited for making such a single-shot approach compatible with the acquisition of 2D NMR data. **Figure 7** illustrates a variety of heteronuclear ultrafast 2D experiments collected on hyperpolarized samples, depicting some of the possibilities that could arise from this integration of single-scan 2D NMR with DNP (63, 64).

Dynamic nuclear polarization (DNP): a generic method to enhance nuclear spin polarizations by saturating the resonances of nearby electrons
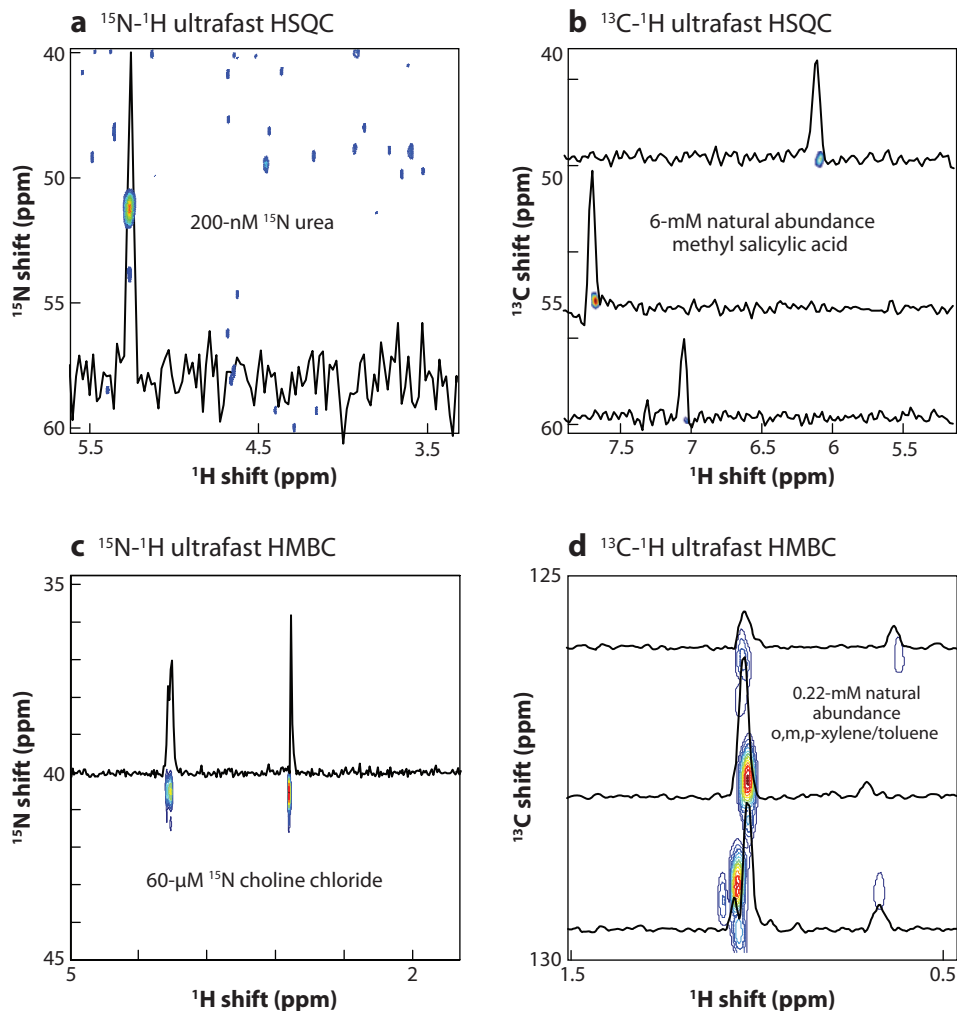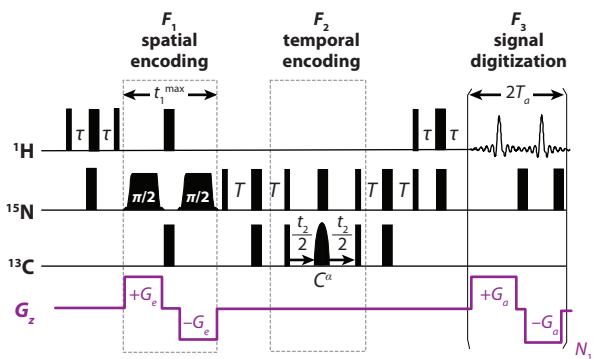
Figure 7

Heteronuclear 2D correlation NMR spectra measured on different dynamic nuclear polarization–enhanced small molecules, showing the compatibility of ultrafast methods with the ex situ liquid-phase hyperpolarization approach. All spectra were measured within 1 s after the sudden dissolution and injection of the targeted molecules, leading to the indicated final effective concentrations. HMBC, heteronuclear multiple-bond correlation; HSQC, heteronuclear single-quantum coherence experiments.

4. EXTENDING ULTRAFAST 2D NUCLEAR MAGNETIC RESONANCE TO HIGHER DIMENSIONALITIES

Higher-dimensional spectroscopy extends the principles embodied in Equation 2, through the addition of an extra mixing process and an additional indirect domain (7, 65). As an example, 3D NMR must deal with the independent incrementation of two indirect-domain time variables, t_1 and t_2, each followed by fixed sequences $Mixing_1$ and $Mixing_2$, respectively, concluding with data acquisition as a function of a direct-domain time t_3. The need to increment two nested indirect-domain delays raises even further challenges in terms of the minimum times required to

a Hybrid 3D pulse sequence

b 3D HNCO 2-mM U-^{13}C/^{15}N LAF
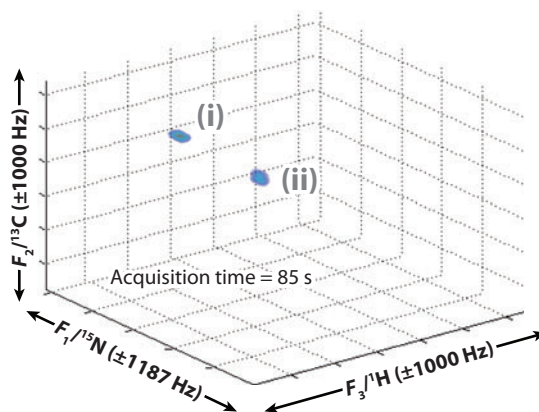
Figure 8

(*a*) Pulse sequence assayed for the accelerated acquisition of 3D HNCO spectra, with the ^{15}N dimension spatially encoded along the *z* axis and ^{13}C interactions monitored using a conventional temporal encoding. Data in the resulting ultrafast 2D planes are then suitably rearranged and Fourier transformed along the t_2, t_3 temporal dimensions. Narrow and wide bars denote nonselective $\pi/2$ and π pulses, respectively; also indicated are the frequency-swept spatial-encoding pulses ($\pi/2$ *labels*). All ^{13}C pulses affect the CO resonance region except for a C^α-specific π inversion in the middle of the t_2 evolution (*shaped pulse*) for homonuclear decoupling purposes. (*b*) Experimental 3D spectrum collected with the sequence shown in panel *a* on a uniformly enriched leucine-alanine-phenylalanine peptide solution. For the ^{13}C dimension, $\Delta t_2 = 500$ μs and 16 time increments were used; overall, 64 scans with a recycle delay of 1.3 s were accumulated.

complete the acquisition of these higher-dimensional data sets; this section briefly discusses new opportunities in this area that may arise from the advent of spatial-encoding methods.

The simplest way to incorporate the concepts introduced in Section 2 into a 3D NMR sequence is to spatially encode one of the indirect domains, while retaining a conventional temporal incrementation to monitor the other. The experimental times required for acquiring such 3D NMR data set then correspond to those normally associated with a 2D acquisition, a substantial reduction compared with conventional counterparts. **Figure 8** shows such a hybrid option as applied to the collection of a 3D HNCO NMR data set. Out of the various alternatives, the scheme shown in **Figure 8*a*** incorporates a spatially encoded chemical-shift evolution of ^{1}H-enhanced ^{15}N sites along the sample's *z* axis, while ^{13}C interactions are monitored in a multiscan fashion using a conventional t_2 incrementation. The resulting HNCO spectrum confirms that 3D NMR data indeed can be obtained in this fashion at approximately 2-mM concentration levels on a 500-MHz spectrometer equipped with a conventional room-temperature probe, within approximately 90-s acquisition times (**Figure 8*b***). Similar timescales and concentrations are also amenable when dealing with small proteins (66).

Further accelerations of high-dimensional experiments could arise by combining the single-scan capabilities of ultrafast 2D NMR with methods capable of performing a more efficient scanning of *n*D time domains based on taking a small number of 2D slices within it (19–21). In the context of 3D NMR acquisition, these projection-reconstruction (PR) methods yield an efficient route to the sampling of the indirect-domain evolution domains. PR substitutes the independent incrementation of the (t_1,t_2) times with a limited number of 2D NMR acquisitions involving fixed ratios $\alpha = \tan^{-1}(\frac{t_2}{t_1})$ of these variables. These in turn represent different α-projections of the spectral data within the 3D frequency space, which can yield the full $F_1F_2F_3$ 3D spectrum being sought

HNCO: 3D NMR experiment correlating ^{1}H and ^{15}N peaks of a given amide group with the carbonyl ^{13}C peak belonging to the previous residue

a TOCSY-based 3D UF PR
  n-butyl chloride

b HSQC-based 3D UF PR
 ^{15}N FMOC-Ala/^{15}N FMOC-Val
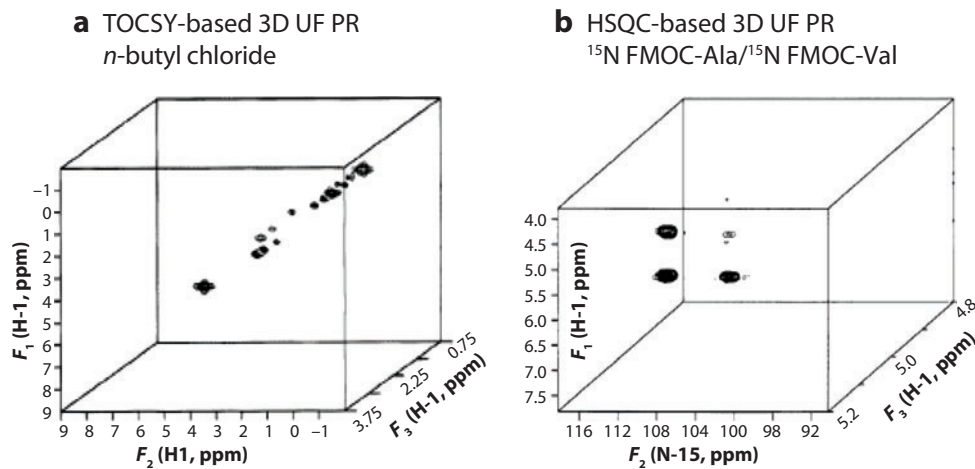
Figure 9

Examples of ultrafast (UF)/projection-reconstruction (PR) 3D NMR acquisitions based on (*a*) homonuclear and (*b*) heteronuclear correlations. Each data set was reconstructed from three single-scan ultrafast 2D projections, leading to a total experimental time of just 5 s (67). HSQC, heteronuclear single-quantum coherence; TOCSY, total correlation spectroscopy.

if inverse-radon-transformed for each discrete direct-domain F_3 frequency. As the individual projected planes needed by this protocol involve the collection of 2D time-domain signals, these in turn can be greatly accelerated by translating the PR principles into the spatio-temporal terms involved in ultrafast NMR. Assuming that the full sample length L is employed when applying these joint indirect-domain (t_1,t_2) encodings, the original PR conditions can be cast into these terms by demanding that the spatio-temporal constants $\{C_i\}_{i=1,2}$ associated with each indirect domain be incremented according to $\alpha = \tan^{-1}(\frac{C_2}{C_1})$ (67). Then, 3D NMR spectra can be recorded by combining a small number of 2D projections, each of which in turn is collected within a single scan. **Figure 9** illustrates this integration with 3D correlation data reconstructed using only three single-scan 2D NMR projections.

Section 2 describes how frequency-swept RF pulses applied in combination with field gradients could be used to spatially encode and subsequently read out the indirect domain of a 2D NMR experiment. Provided that linearly independent gradient geometries are used, these arguments can be extended further to include an arbitrary number of indirect dimensions (24) and thereby to acquire arbitrarily high *n*D NMR data within a single transient. For example, **Figure 10*a*** incorporates two separate gradients arranged along linearly independent z and y geometries to implement the consecutive encodings of the spin evolution that would be needed for a 3D NMR acquisition. The first of these processes induces an $\Omega_1 t_1$-dependent winding of the spin packets along the z direction, whereas for each z coordinate, a second gradient generates an $\Omega_2 t_2$-dependent encoding along the y axis. Because of the ensuing double-winding of spin packets, the overall bulk magnetization is reduced again to zero, and an acquisition process implemented on the resulting sample is associated with a null initial signal. Moreover, only the simultaneous application of suitable G_a^z, G_a^y acquisition gradients can succeed in aligning the spin packets throughout the sample's volume, leading to a definition of the peak's indirect-domain frequencies as a function of two independent variables: $k_z/C_z \propto \int G_a^z(t)dt(L_z/t_1^{\max})$ and $k_y/C_y \propto \int G_a^y(t)dt(L_y/t_2^{\max})$. Oscillation of these two wave numbers as a function of a direct-domain acquisition time t_3 yields a rasterization of the 3D $F_1 F_2 t_3$ mixed domain, and 1D FT as a function of t_3 can thereby provide the full set of peak

a 3D HNCO with full spatial encoding
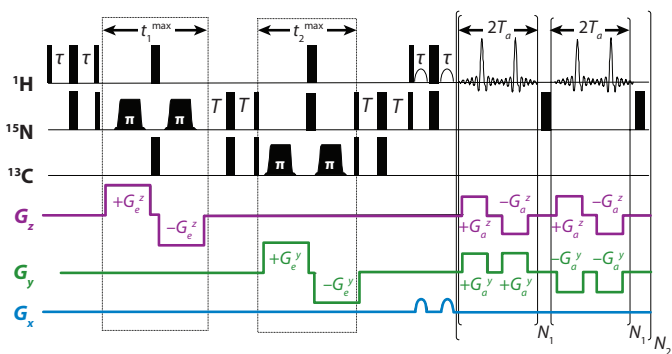
b 3D HNCO 2-mM U-^{13}C/^{15}N LAF
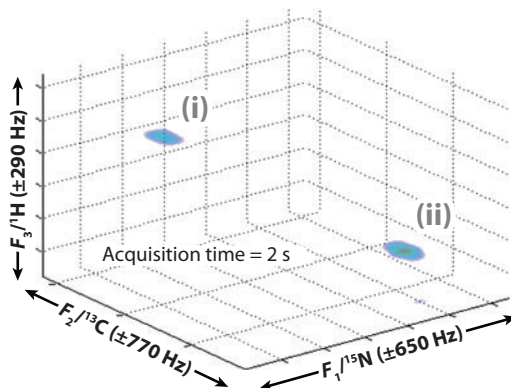
Figure 10

(*a*) 3D ultrafast HNCO based on a pulse sequence involving spatial encoding of ^{15}N (F_1) along the *z* axis and ^{13}C (F_2) along the *y* axis. (*b*) Data set collected on U-^{15}N/^{13}C LAF in d$_6$-DMSO/H$_2$O in only two scans (for the sake of phase cycling away artifacts) on an 800-MHz spectrometer using a room-temperature probe.

coordinates along all the 3D spectral coordinates for all intervening sites—within a single scan. The resulting approach suffers from an even further decrease in sensitivity over its 2D counterpart because of its need to concomitantly sample multiple spectral domains per dwell along the direct time domain. Nevertheless, if sensitivity is sufficient, a dramatic reduction in the overall acquisition time required for completing a 3D NMR experiments can be achieved. **Figure 10*b*** illustrates this for a 3D HNCO example on the same peptide that was analyzed in **Figure 8**; this time, only a couple of phase-cycled scans lead to the desired trace in an approximately 2-s overall acquisition (66).

5. ADDITIONAL SPECTROSCOPIC OPPORTUNITIES PROVIDED BY SPATIALLY SELECTIVE MANIPULATIONS

Similar to its NMR imaging counterpart, ultrafast NMR operates under the presence of extensive magnetic field gradients. In contrast to MRI-oriented methods seeking to obtain spatially resolved information, however, the techniques described above look for a purely spectroscopic, coherent NMR evolution. Still, we believe that these applications within an *n*D NMR context constitute just part of the potential of these novel concepts. Indeed, in addition to a variety of applications demonstrated in MRI-oriented experiments (68–71), spatial encoding has also been used to speed up other types of purely spectroscopic NMR measurements that—although not necessarily monitoring a coherent indirect-domain evolution—still demand the acquisition of a series of spectra for their execution. This section briefly surveys some of these instances.

A well-known example of a measurement requiring multiscan acquisitions is the inversion-recovery experiment, which aims to measure the spin-lattice relaxation time T_1 (2, 7). This method monitors signals arising upon subjecting spins to a delay-180°-τ-90° sequence, as a function of various τ values. The most time-consuming step in this kind of experiment is the initial recycle delay, during which the magnetization is expected to recover to its full equilibrium value after waiting for an a priori unknown delay, $\geq 5T_1$. By replacing the final 90° hard pulse with a spatially selective excitation coupled to a single-scan data-acquisition period, this experiment can be compressed from an array into a single scan (72). In the resulting single-scan inversion-recovery sequence, a single 180° pulse is thus required to invert the full magnetization; as magnetization relaxes back
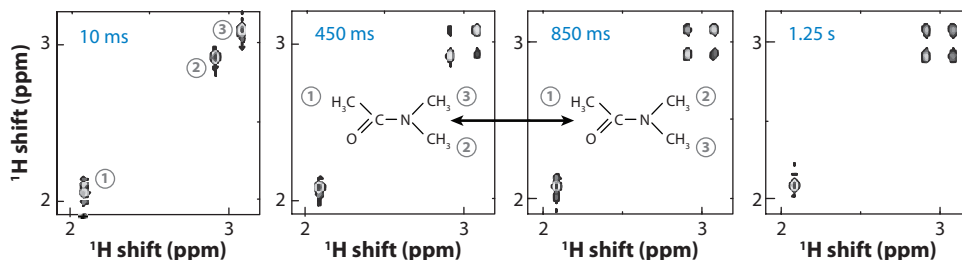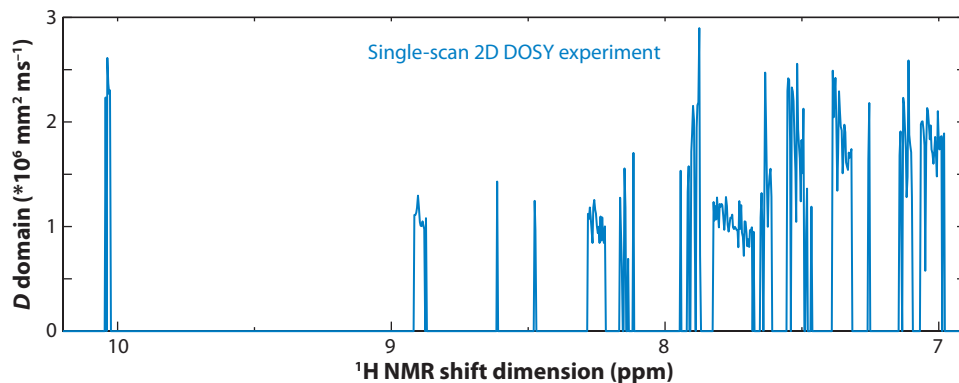
Figure 11

Array of single-scan 2D exchange NMR spectra collected on a dimethylacetamide/D_2O solution as a function of the indicated mixing periods. All these 2D spectra rely on a common initial spatial-encoding process along the sample's z axis; each spectrum was then recalled and measured following different exchange delays, using 90° final excitation pulses and selecting different planes along the sample's x direction. The time required to collect each of the 2D NMR experiments was 66 ms plus the indicated duration of the mixing times; the acquisition of the full series of 2D NMR spectra required only 1.499 s, including all the nested mixing delays (73).

to equilibrium, different slices of the sample are then successively excited and probed as a function of different recovery durations τ—thus completing the measurement of the full array in a single transient. A somewhat similar idea, incorporating an array of a 2D set of exchange experiments as a function of varying mixing periods (73), has also been demonstrated in this fashion. **Figure 11** illustrates how, in very short acquisition times, the effects of chemical exchange can be clearly followed by the growth of the ensuing off-diagonal exchange-derived cross peaks.

Another spatial manipulation principle that—although it does not include the encoding of spin coherences—also compresses an arrayed acquisition into a single scan has been discussed recently in connection with the 2D diffusion ordered spectroscopy experiment (74, 75). This shift-resolved characterization of molecular diffusion is used widely, among other applications, for separating NMR peaks according to the individual chemical components partaking of a complex mixture and for extracting the approximate hydrodynamic radii of molecules in solution (76–78). A suitable application of swept pulses and refocused gradients also manages, in this case, to impart along a sample's axis an array of diffusion-dependent q-encoding values of the kind needed to extract a full 2D diffusion ordered spectroscopy spectral set. **Figure 12** summarizes the type of results that can become available by this single-scan methodology.

An additional example of how spatial-encoding strategies can be exploited to compress what usually entails a series of different scans into a single transient has been demonstrated recently within the context of the phase cycling of RF pulses for coherence selection and/or artifact suppression purposes. Phase cycling is particularly onerous scan-wise within the context of conventional 2D acquisitions, given the large number of pulses involved, the numerous coherence transfer pathways thus potentially created, and the need to couple their suitable filtration to the sampling of numerous incremented indirect-domain evolution delays (2, 7). It is consequently particularly attractive to employ spatially selective strategies to compress complex cycling schemes effectively into a single scan. The feasibility of this approach was demonstrated by the implementation of the various RF manipulations that would normally be executed throughout the independent step of the cycling scheme, at once and throughout different positions along the sample. The joint detection of the signals from all slices and their suitable combination could then yield the desired coherence pathway contributions to the final observable signal (79). In another development related to artifact suppression in high-resolution 2D NMR, spatially selective manipulations have been applied to eliminate zero-quantum coherence (ZQC) contributions often arising upon executing

Figure 12

Single-scan 2D diffusion ordered spectroscopy (DOSY) behavior observed for a mixture of tetraphenyl-porphine, benzaldehyde, and diphenylether ($\approx$50 mM each) in CDCl$_3$ at 25°C. The horizontal axis corresponds to the high-resolution trace afforded by this sequence along the ^{1}H dimension; the vertical axis measures the diffusion coefficients extracted for each peak in the spectrum as a function of chemical shift. Notice the clear separation between the slower diffusivity shown by the porphyrin molecule peaks ($D \approx 1.2 \times 10^{-6}$ mm^2 ms^{-1}) and the remaining, smaller aromatic molecules (75).

2D nuclear Overhauser enhancement spectroscopy–type NMR sequences. These experiments are challenged by difficulties in differentiating longitudinal M_z-type magnetizations and/or spin-order states from ZQCs—given that both behave identically when subject to conventional phase-cycling or gradient-purging procedures. Conversely, the action of a frequency-swept 180° pulse in the presence of a magnetic field gradient enables one to eliminate ZQC-derived artifacts while retaining the remaining longitudinal components because of the destructive interference between ZQC contributions that then derive from different parts in the sample (80, 81).

6. CONCLUDING REMARKS

This review presents the basic principles of and some opportunities that could arise from recently proposed NMR spatial-encoding procedures, particularly for compressing what would normally require the collection of multiple 1D NMR spectra, into a single scan. One main feature of this MRI-derived approach to spectroscopy is that, inasmuch as nD NMR acquisitions are concerned, it is general: Therefore, provided that sufficient sensitivity is available, it can be applied to acquire a variety of homo- and heteronuclear 2D NMR spectra within a single scan. The availability of a protocol capable of delivering such rich information within short timescales could thus benefit certain chemical and biological studies that have hitherto been impractical with the aid of 2D spectroscopy. Potential applications discussed within this context include the use of 2D NMR as a real-time tool for following chemical and biophysical processes, for monitoring the fingerprints of samples undergoing continuous flow, and for exploiting the sensitivity that can be provided by single-shot nuclear hyperpolarization methods. A number of spectroscopic extensions of these ideas are also discussed, including their use in accelerating higher-dimensional ($\geq$3D) NMR experiments; in speeding up diffusion, exchange, and relaxation measurements; and in accelerating and perfecting the elimination of spectral artifacts.

Despite the exiting new opportunities that arise when considering the various applications of these concepts, we stress that these benefits can only materialize in practice if there is sufficient spectral sensitivity. Indeed, whereas spatial encoding enables the compression of a wide variety

of arrayed NMR experiments into a single scan, useful results can only be extracted from such acquisitions if there is sufficient sensitivity to observe the desired information. In this respect, on a per-scan basis, ultrafast nD NMR methods prove less sensitive than conventional counterparts because of their need to rapidly sample multiple dimensions at once. This in turn brings about a need to further expand the NMR's receiver bandwidth, thereby causing an increase in the incoming spectral noise. All this highlights the importance of enhancing sensitivity as a major goal to focus on, if intending to bring out the full potential of these accelerated acquisition methods.

SUMMARY POINTS

1. Imaging-derived concepts can be used to encode the time evolution normally undergone by spins over the course of an NMR experiment, along a spatial domain.

2. This spatial-encoding approach enables the compression of arrayed NMR acquisitions, particularly those involved in multidimensional NMR experiments, into a single scan.

3. This compression enables the reduction of the overall acquisition times of arbitrary homo- or heteronuclear 2D NMR experiments by several orders of magnitude, resulting in an ultrafast approach to multidimensional spectroscopy that may enable new applications in chemical, biophysical, and in vivo NMR.

4. Among the possible applications for this new acquisition mode are real-time 2D NMR measurements of analytes subject to continuous flow, the following of transient chemical and biophysical rearrangements, 2D measurements on hyperpolarized samples, and extensions to higher-dimensional experiments.

5. The success of these new potential applications hinges on the ability of achieving sufficient sensitivity to observe the desired multidimensional NMR signals within a single, or at most a few, transients.

DISCLOSURE STATEMENT

The authors are not aware of any biases that might be perceived as affecting the objectivity of this review.

ACKNOWLEDGMENTS

LITERATURE CITED

1. Grant DM, Harris RK, eds. 1996. *Encyclopedia of NMR*. Chichester, NY: Wiley & Sons
2. Derome AE. 1987. *Modern NMR Techniques for Chemistry Research*. Oxford: Pergamon
3. Frydman L. 2001. Perspectives in solid state NMR: spin-1/2 and beyond. *Annu. Rev. Phys. Chem.* 52:463–98
4. Cavanagh J, Fairbrother WJ, Palmer AG, Skelton NJ. 1996. *Protein NMR Spectroscopy: Principles and Practice*. San Diego: Academic

5. deGraaf R. 2007. *In Vivo NMR Spectroscopy: Principles and Techniques*. Chichester, NY: Wiley & Sons

6. Buxton RB. 2001. *An Introduction to Functional MRI: Principles and Techniques*. Cambridge: Cambridge Univ. Press

7. Ernst RR, Boudenhausen G, Wokaun A. 1987. *Principles of Nuclear Magnetic Resonance in One and Two Dimensions*. Oxford: Clarendon

8. Ernst RR, Anderson WA. 1966. Application of Fourier transform spectroscopy to magnetic resonance. *Rev. Sci. Instrum.* 37:93–102

9. Jeener J. 1994 (1971). Ampere Summer School lecture notes. In *NMR and More in Honor of Anatole Abragam*, ed. M Goldman, M Porneuf, pp. 1–379. Les Ulis, France: Ed. Phys.

10. Aue WP, Bartholdi E, Ernst RR. 1976. Two dimensional spectroscopy: application to nuclear magnetic resonance. *J. Chem. Phys.* 64:2229–46

11. Kupče E, Nishida T, Freeman R. 2003. Hadamard NMR spectroscopy. *Prog. Nucl. Magn. Reson. Spectrosc.* 42:95–122

12. Atreya HS, Szyperski T. 2005. Rapid NMR data collection. *Methods Enzymol.* 394:78–108

13. Mandelshtam VA. 2000. The multidimensional filter diagonalization method I. Theory and numerical implementation. *J. Magn. Reson.* 144:343–56

14. Hoch JC, Stern AS. 2001. Maximum entropy reconstruction, spectrum analysis and deconvolution in multidimensional nuclear magnetic resonance. *Methods Enzymol.* 338:159–78

15. Orekhov Y, Ibraghimov I, Billeter M. 2003. Optimizing resolution in multidimensional NMR by three-way decomposition. *J. Biomol. NMR* 27:165–73

16. Brüschweiler R, Zhang F. 2004. Covariance nuclear magnetic resonance spectroscopy. *J. Chem. Phys.* 120:5253–60

17. Kupče E, Freeman R. 2003. Frequency-domain Hadamard spectroscopy. *J. Magn. Reson.* 162:158–65

18. Bodenhausen G, Ernst RR. 1981. The accordion experiment, a simple approach to three-dimensional NMR spectroscopy. *J. Magn. Reson.* 45:367–73

19. Szyperski T, Wider G, Bushweller JH, Wuthrich K. 1993. Reduced dimensionality in triple-resonance NMR experiments. *J. Am. Chem. Soc.* 115:9307–8

20. Kim S, Szyperski T. 2003. GFT NMR, a new approach to rapidly obtain precise high-dimensional NMR spectral information. *J. Am. Chem. Soc.* 125:1385–93

21. Kupče E, Freeman R. 2004. Projection-reconstruction technique for speeding up multidimensional NMR spectroscopy. *J. Am. Chem. Soc.* 126:6429–40

22. Frydman L, Scherf T, Lupulescu A. 2002. The acquisition of multidimensional NMR spectra within a single scan. *Proc. Natl. Acad. Sci. USA* 99:15858–62

23. Frydman L, Scherf T, Lupulescu A. 2003. Principles and features of single-scan two-dimensional NMR spectroscopy. *J. Am. Chem. Soc.* 125:9204–17

24. Shrot Y, Frydman L. 2003. Single-scan NMR spectroscopy at arbitrary dimensions. *J. Am. Chem. Soc.* 125:11385–96

25. Pelupessy P. 2003. Adiabatic single scan two-dimensional NMR spectroscopy. *J. Am. Chem. Soc.* 125:12345–50

26. Shrot Y, Shapira B, Frydman L. 2004. Ultrafast 2D NMR spectroscopy using continuous spatial encoding of the spin interactions. *J. Magn. Reson.* 171:163–70

27. Tal A, Shapira B, Frydman L. 2005. A continuous phase-modulated approach to spatial encoding in ultrafast 2D NMR spectroscopy. *J. Magn. Reson.* 176:107–14

28. Andersen NS, Köckenberger W. 2005. A simple approach for phase-modulated single-scan 2D NMR spectroscopy. *Magn. Reson. Chem.* 43:795–97

29. Shapira B, Shrot Y, Frydman L. 2006. Symmetric spatial encoding in ultrafast 2D NMR spectroscopy. *J. Magn. Reson.* 178:33–41

30. Giraudeau P, Akoka S. 2007. A new detection scheme for ultrafast 2D J-resolved spectroscopy. *J. Magn. Reson.* 186:352–57

31. Shrot Y, Frydman L. 2008. Spatial encoding strategies for ultrafast multidimentional nuclear magnetic resonance. *J. Chem. Phys.* 128:052209

32. Lindon JC, Holmes E, Nicholson JK. 2004. Toxicological applications of magnetic resonance. *Progr. Nucl. Magn. Reson. Spectrosc.* 45:109–43

33. Albert K, ed. 2002. *On-Line LC-NMR and Related Techniques*. Chichester, NY: Wiley & Sons

34. Braunschweiler L, Ernst RR. 1983. Coherence transfer by isotropic mixing: applications to proton correlation spectroscopy. *J. Magn. Reson.* 53:521–28

35. Shapira B, Karton A, Aronzon D, Frydman L. 2004. Real-time 2D NMR identification of analytes undergoing continuous chromatographic separation. *J. Am. Chem. Soc.* 126:1262–65

36. Dayie KT, Wagner G, Lefèvre J-F. 1996. Theory and practice of nuclear spin relaxation in proteins. *Annu. Rev. Phys. Chem.* 47:242–83

37. Bain AD. 2003. Chemical exchange in NMR. *Prog. Nucl. Magn. Reson. Spectrosc.* 43:63–103

38. Dobson CM, Hore PJ. 1998. Kinetic studies of protein folding using NMR spectroscopy. *Nat. Struct. Biol.* 5:504–7

39. Ishima R, Torchia DA. 2000. Protein dynamics from NMR. *Nat. Struct. Biol.* 7:740–43

40. Gal M, Mishkovsky M, Frydman L. 2006. Real-time monitoring of chemical transformation by ultrafast 2D NMR spectroscopy. *J. Am. Chem. Soc.* 128:951–56

41. Müller L. 1979. Sensitivity enhanced detection of weak nuclei using heteronuclear multiple quantum coherence. *J. Am. Chem. Soc.* 101:4481–84

42. Schanda P, Brutscher B. 2005. Very fast two-dimensional NMR spectroscopy for real-time investigation of dynamic events in proteins on the time scale of seconds. *J. Am. Chem. Soc.* 127:8014–15

43. Pervushin K, Voegeli B, Eletsky A. 2002. Longitudinal ^{1}H relaxation optimization in TROSY NMR spectroscopy. *J. Am. Chem. Soc.* 124:12898–902

44. Freeman R, Hill HDW. 1971. Phase and intensity abnormalities in Fourier transform NMR. *J. Magn. Reson.* 4:366–83

45. Ross A, Salzmann M, Senn H. 1997. Fast-HMQC using Ernst angle pulses: an efficient tool for screening of ligand binding to target protein. *J. Biomol. NMR* 10:289–96

46. Gal M, Schanda P, Brutsher B, Frydman L. 2007. UltraSOFAST HMQC NMR and the repetitive acquisition of 2D protein spectra at Hz rates. *J. Am. Chem. Soc.* 129:1372–77

47. Bowers CR, Weitekamp DP. 1986. Transformation of symetrization order in nuclear magnetic resonance. *Phys. Rev. Lett.* 57:2645–48

48. Eisenschmid TC, Kirss RU, Deutsch PP, Hommeltoft SI, Eisenberg R, et al. 1987. Parahydrogen induced polarization in hydrogenation reaction. *J. Am. Chem. Soc.* 109:8089–91

49. Albert MS, Cates GD, Driehuys B, Happer W, Saam B, et al. 1994. Biological magnetic resonance imaging using laser polarized ^{129}Xe. *Nature* 370:199–201

50. Navon G, Song YQ, Room T, Appelt S, Taylor RE, Pines A. 1996. Enhancement of solution NMR and MRI with laser polarized xenon. *Science* 271:1848–51

51. Muus LT, Atkins PW, McLauchlen KA, Pedersen JB. 1977. *Chemically Induced Magnetic Polzarization*. Dordrecht: D. Reidel

52. Shapira B, Morris E, Muszkat KA, Frydman L. 2004. Sub-second 2D NMR spectroscopy at submilimolar consentrations. *J. Am. Chem. Soc.* 126:11756–57

53. Carver TR, Slichter CP. 1953. Polarization of nuclear spin in metals. *Phys. Rev.* 92:212–13

54. Hausser KH, Stehilk D. 1968. Dynamic nuclear polarization in liquids. *Adv. Magn. Reson.* 3:79–139

55. Abragam A, Goldman M. 1982. *Nuclear Magnetism: Order and Disorder*. Oxford: Oxford Univ. Press

56. Ardenkjaer-Larsen JH, Fridlund B, Gram A, Hansson G, Hansson L, et al. 2003. Increase in signal-to-noise ratio of >10,000 times in liquid-state NMR. *Proc. Natl. Acad. Sci. USA* 100:10158–63

57. Joo CG, Hu KN, Bryant JA, Griffin RG. 2006. In situ temperature jump high-frequency dynamic nuclear polarization experiments: enhanced sensitivity in liquid-state NMR spectroscopy. *J. Am. Chem. Soc.* 128:9428–32

58. Golman K, Ardenkjær-Larsen JH, Petersson JS, Månsson S, Leunbach I. 2003. Molecular imaging with endogenous substances. *Proc. Natl. Acad. Sci. USA* 100:10435–39

59. Golman K, Zandt R, Thaning M. 2006. Real time metabolic imaging. *Proc. Natl. Acad. Sci. USA* 103:11270–75

60. Chen AP, Albers MJ, Cunningham CH, Kohler SJ, Yen YF, et al. 2007. Hyperpolarized C-13 spectroscopic imaging of the TRAMP mouse at 3T: initial experience. *Magn. Reson. Med.* 58:1099–106

61. Day SE, Kettunen MI, Gallagher FA, Hu DE, Lerche M, et al. 2007. Detecting tumor response to treatment using hyperpolarized ^{13}C magnetic resonance imaging. *Nat. Med.* 13:1382–87

62. Gallagher FA, Kettunen MI, Day SE, Hu DE, Ardenkjaer-Larsen JH, et al. 2008. Magnetic resonance imaging of pH in vivo using hyperpolarized ^{13}C-labelled bicarbonate. *Nature* 457:940–43

63. Frydman L, Blazina D. 2007. Ultrafast two-dimensional nuclear magnetic resonance spectroscopy of hyperpolarized solutions. *Nat. Phys.* 3:415–19

64. Mishkovsky M, Frydman L. 2008. Progress in hyperpolarized ultrafast 2D nuclear magnetic resonance. *Chem. Phys. Chem.* 16:2340–48

65. Sattler M, Schleucher J, Griesinger C. 1999. Heteronuclear multidimensional NMR experiments for the structure determination of proteins in solution employing pulsed field gradients. *Progr. Nucl. Magn. Reson. Spectrosc.* 34:93–158

66. Mishkovsky M, Gal M, Frydman L. 2007. Spatially-encoded strategies in the execution of biomolecular-oriented 3D NMR experiments. *J. Biomol. NMR* 39:291–301

67. Mishkovsky M, Kupce E, Frydman L. 2007. Ultrafast based projection-reconstruction three-dimensional nuclear magnetic resonance spectroscopy. *J. Chem. Phys.* 127:034507

68. Shrot Y, Frydman L. 2005. Spatially-encoded NMR and the acquisition of 2D magnetic resonance images within a single scan. *J. Magn. Reson.* 172:179–90

69. Tal A, Frydman L. 2006. Spatial encoding and the acquisition of high definition MR images in inhomogeneous magnetic fields. *J. Magn. Reson.* 181:179–94

70. Chamberlain R, Park JY, Corum C, Yacoub E, Ugurbil K, et al. 2007. RASER: a new ultrafast magnetic resonance imaging method. *Magn. Reson. Med.* 58:794–99

71. Tal A, Frydman L. 2007. Spectroscopic imaging from spatially-encoded single-scan multidimensional MRI data. *J. Magn. Reson.* 189:46–58

72. Bhattacharyya R, Kumar A. 2003. A fast method for the measurement of long-spin lattice relaxation times by single scan inversion recovery experiment. *Chem. Phys. Lett.* 383:99–103

73. Shapira B, Frydman L. 2003. Arrayed acquisition of 2D exchange NMR spectra within a single experiment. *J. Magn. Reson.* 165:320–24

74. Thrippleton MJ, Loening NM, Keeler J. 2003. A fast method for the measurement of diffusion coefficients: one-dimensional DOSY. *Magn. Reson. Chem.* 41:441–47

75. Shrot Y, Frydman L. 2008. Single scan 2D DOSY NMR. *J. Magn. Reson.* 195:226–31

76. Morris KF, Johnson CS. 1993. Resolution of discrete and continuous molecular-size distributions by means of diffusion-ordered 2D NMR spectroscopy. *J. Am. Chem. Soc.* 115:4291–99

77. Barjat H, Morris GA, Smart S, Swanson AG, Williams SCR. 1995. High-resolution diffusion-ordered 2D spectroscopy (HR-DOSY): a new tool for the analysis of complex mixtures. *J. Magn. Reson. B* 108:170–72

78. Johnson CS. 1999. Diffusion-ordered NMR spectroscopy: principles and applications. *Prog. NMR Spectrosc.* 34:203–55

79. Parish DN, Szyperski T. 2008. Simultaneously cycled NMR spectroscopy. *J. Am. Chem. Soc.* 130:4925–33

80. Thrippleton JM, Keeler J. 2003. Elimination of zero quantum interference in two dimensional NMR spectra. *Angew. Chem. Int. Ed. Engl.* 42:3938–41

81. Cano E, Thrippleton JM, Keeler J, Shaka AJ. 2004. Cascaded z-filters for efficient single-scan suppression of zero-quantum coherence. *J. Magn. Reson.* 167:291–97

**Annual Review of
Physical Chemistry**

Volume 60, 2009

Contents

Indexes

Errata

An online log of corrections to *Annual Review of Physical Chemistry* articles may be
found at http://physchem.annualreviews.org/errata.shtml